Short Communication

Title:

A motion-decomposition approach to address gimbal lock in the 3-cylinder open chain mechanism description of a joint coordinate system at the glenohumeral joint

Authors: Hippolite O Amadi and Anthony MJ Bull

Department of Bioengineering, Imperial College London, South Kensington Campus, London SW7 2AZ, UK

Corresponding Author:

Dr Hippolite O Amadi

Department of Bioengineering

Imperial College London

South Kensington Campus

London SW7 2AZ,

United Kingdom

+44 1708456911

hippolite.amadi00@imperial.ac.uk

Keywords: JCS, Glenohumeral, shoulder, window, gimbal lock, physiological kinematics

Word Count: Abstract (164), text (1998)

No of Figures: 3

Abstract

In this study, the standard-sequence properties of a joint coordinate system were implemented for the glenohumeral joint by the use of a set of instantaneous geometrical planes. These are: a plane that is bounded by the humeral long axis and an orthogonal axis that is the cross product of the scapular *anterior* axis and this long axis, and a plane that is bounded by the long axis of the humerus and the cross product of the scapular *lateral* axis and this long axis. The relevant axes are updated after every decomposition of a motion component of a humeral position. Flexion, Abduction and rotation are then implemented upon three of these axes and are applied in a step-wise uncoupling of an acquired humeral motion to extract the joint coordinate system angles. This technique was numerically applied to physiological kinematics data from the literature to convert them to the joint coordinate system and to visually reconstruct the motion on a set of glenohumeral bones for validation.

1.0 Introduction

The large range of rotation of the glenohumeral joint (GHJ) causes difficulties in biomechanical and kinematic analysis of its function when the full range of motion is required to be analysed. Gimbal lock (Senk and Cheze, 2006; Masuda et al., 2008) is the manifestation of this problem, which for the shoulder joint can occur as a mathematically unstable position of GHJ motion interpretation when the flexion/extension axis and the internal/external rotation axis of the humerus coincide; this is found in the clinical position of 90° GHJ abduction. In order to study the kinematics of shoulder pathologies (range of motion and joint stability) an approach that ameliorates against sequence-dependent eulerian rotations that suffer from gimbal lock must be employed (Kontaxis et al., 2009; Hoffmann, 2002; Karduna et al., 2000). This issue has been addressed in hinge-like joints such as the knee and elbow (Wu et al., 2002) by applying the principles of Grood and Suntay's (1983) 'joint coordinate system' (JCS), which is a Z-X-Y Cardan rotation decomposition with a vectorial approach to quantify translations. However, because no agreed approach for applying this JCS to the GHJ, which is essentially a three degree of freedom spherical joint, has been described in the literature, the ISB have not recommended the use of this JCS at the GHJ (Wu et al., 2005). In fact, it is clear that current opinion generally focuses on using different rotation decompositions dependent on the movement of interest (Senk and Cheze, 2006). It is appealing to devise a way of adapting the Grood-&-Suntay style of JCS to the GHJ that will allow the interpretation of kinematic studies in the literature that have used alternative approaches (Browne et al., 1990; Fung et al., 2001).

Therefore, the aim of this study was to devise and test a technique to adapt the JCS to the GHJ and allow the conversion of kinematics data from the literature into the clinical degrees-of-freedom (DOF) variables of abduction, flexion and rotation.

2.0 Methods

The study was in two parts:

(1) presents a method allowing the ‘Grood and Suntay’ JCS style to be applied to the GHJ and

(2) presents a method of motion decomposition allowing quantification of the DOF JCS variables of any GHJ position.

2.1 JCS at the GHJ

Literature-defined body-fixed axes that are consistent with standard diagnostic shoulder scans were assigned to the humerus and scapula (Amadi, 2006; Amadi et al., 2008; Amadi et al., 2009a). A JCS was defined that consists of the infero-superior axis of the humerus ($\mathbf{u}_{hx}$), the medio-lateral axis of the scapula ($\mathbf{u}_{sz}$) and their mutual orthogonal floating axis ($\mathbf{u}_{f}$) (Figure 1). A guiding concept, mobile-square-window (MSW), was devised to simplify the decomposition process of a GHJ kinematics position in a JCS. $\mathbf{u}_{sz\text{-}orth}$ is the cross product of $\mathbf{u}_{hx}$ and the scapular anterior axis ($\mathbf{u}_{sy}$). This and $\mathbf{u}_{hx}$ form the orthogonal axes that define the MSW plane.

This window captures the original orientation of the humerus and then transforms with it as it rotates and translates. The JCS standardised sequence at the GHJ was evaluated within the mobile-square-window to enable the quantification of the joint’s angles in clinical terms. Hence, GHJ angles of flexion, abduction and rotation were resolved about $\mathbf{u}_{sz\text{-}orth}$, $\mathbf{u}_{f}$ and $\mathbf{u}_{hx}$ respectively (Figure 2).

2.2 GHJ Rotation Variables

The scapular coronal, sagittal and humeral transverse planes (perpendicular to $\mathbf{u}_{\mathbf{sy}}$, $\mathbf{u}_{\mathbf{sz}}$ and, $\mathbf{u}_{\mathbf{hx}}$, respectively) were considered in relation to the special case when the humeral and scapular coordinate frames coincided

(Figure 1b). This is defined as the GHJ 'neutral-position'. By the JCS fundamental definition, the floating axis, scapular $\mathbf{u}_{\mathbf{sy}}$, humeral $\mathbf{u}_{\mathbf{hy}}$ and $\mathbf{u}_{msw}$ would all coincide while $\mathbf{u}_{sz\text{-}orth}$ would coincide with $\mathbf{u}_{sz}$ (Figure 1b). Then in this position, the MSW lies on the coronal plane and so:

(I) Abduction; defined as the coronal plane elevation angle between [$\mathbf{u}_{hx}$] and the scapular sagittal plane, is zero.

(II) Flexion; the sagittal plane elevation angle between MSW-plane and the scapular coronal plane, is also zero.

(III) Internal rotation; the angle of rotation of the humeral lateral axis [$\mathbf{u}_{hz}$] on the transverse plane, i.e. angle between the scapular lateral axis [$\mathbf{u}_{sz}$] and that of the humerus [$\mathbf{u}_{hz}$]. This is also zero.

The above scenario pictures the simplest quantifiable orientation of the GHJ. A complex orientation during function can however be solved if it is broken down to this simple form by a step-wise subtraction of constituting 'flexion', 'abduction' and finally 'internal rotation' (Figure 2). This was achieved by the application of an existing vector rotation algorithm from the literature (Amadi et al., 2009b).

2.3 Motion Decomposition

Uncoupling a GHJ motion would require knowledge of the primary motion, whether predominately flexion or abduction (Figure 1c and 1d).

1 The primary motion was estimated as follows:

   a. Convert $\mathbf{u}_{\mathbf{hx}}$, $\mathbf{u}_{\mathbf{sz}}$ and $\mathbf{u}_{\mathbf{sy}}$ into the glenoid coordinate system such that the vector directions of $\mathbf{u}_{\mathbf{sz}}$ and $\mathbf{u}_{\mathbf{sy}}$ are [1 0 0] and [0 1 0], respectively.

b. If ‘absolute[$\mathbf{u}_{hx}$(x)]’ is greater than ‘absolute[$\mathbf{u}_{hx}$(y)]’ then this is primarily abduction, else flexion.

2 Coupled abduction or flexion was subtracted first before quantifying the primary.

The fundamental variables of rotations at a right GHJ were studied using the defined and derived axes of humerus, scapula and JCS:

(I) Flexion (β); the angle of elevation of the plane of the MSW about $\mathbf{u}_{sz\text{-}orth}$ (Figure 2a). This is therefore a measure of the angle “β” between the normal to MSW ($\mathbf{u}_{msw}$) and the normal to the scapular coronal plane ($\mathbf{u}_{sy}$) (Figure 2b). Flexion was decomposed by extension of $\mathbf{u}_{hx}$ about $\mathbf{u}_{sz\text{-}orth}$ through β° to assume a new orientation $\mathbf{u}_{hxa}$ (Figure 2c).

(II) Abduction (θ); which is the elevation of the humeral long axis on the plane of the MSW and about the normal to the window (Figure 2c). This, therefore, measures the angle “θ” between ($\mathbf{u}_{hxa}$) and the scapular superior axis ($\mathbf{u}_{sx}$). GHJ abduction angle was decomposed by adducting $\mathbf{u}_{hxa}$ about $\mathbf{u}_{sy}$ through θ° to assume the same orientation as $\mathbf{u}_{sx}$. This results in a new $\mathbf{u}_{sz\text{-}orth}$ orientation that coincides with $\mathbf{u}_{sz}$.

(III) Internal rotation (γ); the degree of humeral rotation about its long axis ($\mathbf{u}_{hx}$). This is a measure of the angle between the humeral ($\mathbf{u}_{hz}$) and scapular ($\mathbf{u}_{sz}$) lateral axes when coupled flexion and abduction of the humerus have been removed from $\mathbf{u}_{hz}$. To achieve this, the flexion decomposition rule, step (I), was imposed on the initially quantified $\mathbf{u}_{hz}$ (i.e. rotating $\mathbf{u}_{hz}$ about $\mathbf{u}_{sz\text{-}orth}$ through β°). The new orientation so obtained was further subjected to the abduction decomposition rule, step (II), to obtain a transverse plane orientation $\mathbf{u}_{hz\text{-}temp}$ (Figure 2d).

Finally, $\mathbf{u}_{hz\text{-}temp}$ was rotated about $\mathbf{u}_{sx}$ through γ° to decompose internal rotation and bring the humeral frame to full alignment with the scapular frame.

A check on the accuracy of the procedure was performed by the imposition of the three decomposition rules upon the original humeral anterior axis [$\mathbf{u}_{hy}$]. These rules were rotations through angles β, θ and γ about the axes $\mathbf{u}_{sz\text{-}orth}$, $\mathbf{u}_{sy}$, and $\mathbf{u}_{sx}$ respectively. For the procedure to be accurate, the final position of the humeral anterior axis [$\mathbf{u}_{hy}$] must be on the sagittal plane and must be equal to the scapular anterior axis [$\mathbf{u}_{sy}$], in orientation.

2.4 Algorithm testing and validation

The validity of the developed algorithm depends on how accurately a known physiological motion can be recreated using it. The algorithm was hence applied to interpret the kinematics of a set of GHJ activities obtained from the literature (Fung et al., 2001). Fung et al (2001) used the Euler Cardan rotation matrix approach to quantitatively study shoulder kinematics in five cadaveric specimens during humeral elevation in three planes to determine the dynamic coupled rotations of the scapula and the clavicle. Their published raw data was applied to the Visible Human Female (VHF) glenohumeral bone set (National Library of Medicine, http://www.nlm.nih.gov/research/visible/visible_human.html) using Euler's sequence as applied by Fung et al as follows:

1. For each arm elevation of Fung et al's experiment, all their fundamental axes were quantified on the VHF bones. Their kinematics variables were applied to a vector rotation algorithm

(Amadi et al., 2009b). This recreated the instantaneous relative bone orientations in their experiment.

2. The recreated orientation was applied to the present algorithm to quantify its constituting JCS clinical variables of abduction, flexion and rotation.
3. The bearing of the recreated humeral long axis from the coronal plane of the VHF image was quantified to verify the swinging alignment of the humerus during each range of motion (ROM).
4. The quantified JCS variables for each ROM were applied as input to a MSW-based kinematics reconstruction tool from the literature (Amadi et al., 2009b). This re-produced a visual perception of the planar elevations in Fung et al's experiment.

3.0 Results

The GHJ JCS reconstruction of the humeral long axis of Fung et al's coronal-plane arm elevation shows that the swinging trajectory travelled on a course 5.5° ± 32.5° to the anatomical coronal plane (Table 1). During scapular and sagittal planes arm elevation, this took the course 36.6° ± 7.0° and 73.0° ± 1.4°, respectively. Figure 3 shows that passive elevation of the arm in any of the three experimented planes results into various degrees of coupled GHJ rotational motions. This interprets Fung et al's 90° arm elevation in the sagittal plane, for example, as GHJ humeral 79.3° flexion plus 44° abduction plus 24.9° internal rotation. The method was further tested in a MSW-based kinematics reconstruction tool to reproduce such GHJ orientations using different clinical sequences (flexion-abduction-rotation, abduction-flexion-rotation, rotation-flexion-abduction), all resulting in the same end point (Amadi et al., 2009b).

4.0 Discussion

The quantified JCS equivalents of the GHJ coupled rotational motions resulting from each instantaneous arm elevation as shown in Figure 3 can only make clinical sense if interpreted with a gimbal-lock-free kinematics tool. It has been argued in the literature that the complexities of the GHJ limit the application of the principles of Grood-&-Suntay's JCS to it (Wu et al., 2005). The International Society of Biomechanics (ISB) therefore recommended the continued application of Euler rotations for the kinematics of the GHJ. Senk and Cheze (2006) tested the gimbal-lock effect whilst putting amplitude of arm motions into account on possible Euler's sequences including the ISB recommendations. They reported that no tested rotation sequence was found to be clinically interpretable for all tested movements. The Grood & Suntay's style of JCS is a better technique in the description of joint relative motion (Dunning et al., 2003, Hill et al., 2008). This is because the standardised sequence property of this JCS makes it clinically easy to use in describing physiological motions. The robust idea of this JCS was therefore desirable to be tweaked for the study of a complex joint such as the GHJ.

In the present work, the concept of a 'mobile-square-window' has been introduced to achieve the quantification and decoupling of associated JCS angles at the GHJ in clinical terms. A motion decomposition algorithm that quantifies the kinematics variables of the JCS for a given instantaneous position of the GHJ was developed and was applied to convert kinematics data from the literature into the JCS clinical variables for reconstruction and further studies (Amadi et al., 2009b; Fung et al., 2001). In a previous work, Brenneke et al interpreted 90° coronal plane arm elevation as constituting an estimated 60° of GHJ abduction (Brenneke et al., 2000; Barnett et al., 1999). However our MSW interpretation for this humeral orientation is 75°, difference stemming from variation between Fung's and Barnettt's results as these reported approximately 18° and 27° of coupled scapular lateral rotation at 90° arm elevation, respectively. The system remained mathematically stable even when extreme cases of GHJ clinical manoeuvres that could otherwise result in gimbal-lock were applied to it (previously shown in Amadi, 2006). This includes interpretation of the GHJ motion at the position where the humeral-$\mathbf{u}_{hx}$ and scapular-$\mathbf{u}_{sz}$ axes overlap.

Further work would require this tool to be tested for joint translations. This would require better knowledge from the literature on the magnitude of these translations which are considered to be of the order of millimetres (Nishinaka et al., 2008).

References

Amadi, H.O., 2006. Glenohumeral joint kinematics and ligament loading. PhD. thesis, Imperial College London.

Amadi, H.O., Hansen, U.N., Wallace, A.L., Bull, A.M.J., 2008. A scapular coordinate frame for clinical and kinematic analyses. Journal of Biomechanics 41, 2144-2149.

Amadi, H.O., Majed, A., Emery, R.J.H., Bull, A.M.J., 2009a. A humeral coordinate system for in vivo 3-D kinematics of the glenohumeral joint. Journal of Musculoskeletal Research 12, 169-174.

Amadi, H.O., Hansen, U.N., Bull, A.M.J., 2009b. A numerical tool for the reconstruction of the physiological kinematics of the glenohumeral joint. Proc. IMechE Part H: Journal of Engineering in Medicine 233(H), 833-837.

Barnett, N.D., Duncan, R.D., Johnson, G.R., 1999. The measurement of three dimensional scapulohumeral kinematics - a study of reliability. Clinical Biomechanics 14, 287-290.

Brenneke, S.L., Reid, J., Ching, R.P., Wheeler, D.L., 2000. Glenohumeral kinematics and capsulo-ligamentous strain resulting from laxity exams. Clinical Biomechanics 15, 735-742.

Browne, A.O., Hoffmeyer, P., Tanaka, S., An, K.N., Morrey, B.F., 1990. Glenohumeral elevation studied in three dimensions. Journal of Bone and Joint Surgery 72-B, 843-845.

Dunning, C.E., Duck, T.R., King, G.J.W., Johnson, J.A., 2003. Quantifying translations in the radiohumeral joint: application of a floating axis analysis. Journal of Biomechanics 36, 1219-1223.

Endo, K., Yukata, K., Yasui, N., 2004. Influence of age on scapulo-thoracic orientation. Journal of Clinical Biomechanics 19, 1009-1013.

Fung, M., Kato, S., Barrance, P., Elias, J., McFarland, E., Nobuhara, K., Chao, E., 2001. Scapular and clavicular kinematics during humeral elevation: A study with cadavers. Journal of Shoulder and Elbow Surgery 10, 278-285.

Gagey, O., Gagey, N., 2001. The hyperabduction test. An assessment of the laxity of the inferior glenohumeral ligament. Journal of Bone and Joint Surgery 82-B, 68-74.

Graichen, H., Stammberger, T., Bonel, H., Haubner, M., Englmeier, K., Reiser, M., et al., 2000. Magnetic resonance based motion analysis of the shoulder during elevation. Clinical Orthopaedics and Related Research 370, 154-163.

Grood, E., Suntay, W., 1983. A joint coordinate system for the Clinical Description of Three-Dimensional Motions: Application to the knee. Trans ASME Journal of Biomechanical Engineering 105,136-144.

Hill, A.M., Bull, A.M.J., Wallace, A.L., Johnson, G.R., 2008. Qualitative and quantitative descriptions of glenohumeral motion. Gait & Posture 27, 177-188.

Hoffmann G., 2002. Infamous gimbal lock. http://www.fho-emden.de/~hoffmann/gimbal09082002.pdf, accessed 6th March 2009.

Hsu, A., Ho, L., Ho, S., Hedman, T., 2000. Joint position during anterior-posterior glide mobilization: Its effect on glenohumeral abduction range of motion. Archives of Physical Medicine and Rehabilitation 81, 210-214.

Karduna, A.R., McClure, P.W., Michener, L.A., 2000. Scapular kinematics: effects of altering the Euler angle sequence of rotations. Journal of Biomechanics 33, 1063-1068.

Kontaxis, A., Cutti, A.G., Johnson, G.R., Veeger, H.E.J., 2009. A frame work for the definition of standardized protocols for measuring the upper-extremity kinematics. Journal of Clinical Biomechanics 24, 246-253.

Koontz, A.M., Cooper, R.A., Boninger, M.L., Souza, A.L., Fay, B.T., 2004. Scapular range of motion in a quasi-wheelchair push. International Journal of Industrial Ergonomics 33, 237-248.

Masuda, T., Ishida, A., Cao, L., Morita, S., 2008. A proposal for a new definition of the axial rotation angle of the shoulder joint. Journal of Electromyography and Kinesiology 18, 154-159.

Nishinaka N, Tsutsui H, Mihara K, Suzuki K, Makiuchi D, Kon Y, Wright TW, Moser MW, Gamada K, Sugimoto H, Banks SA., 2008. Determination of in vivo glenohumeral translation using fluoroscopy and shape-matching techniques. Journal of Shoulder and Elbow Surgery 17, 319-322.

Novotny, J., Beynnon, B., Nichols, C., 2000. Modeling the stability of the glenohumeral joint during external rotation. Journal of Biomechanics 33, 345-354.

Senk, M., Cheze, L., 2006. Rotation sequence as an important factor in shoulder kinematics. Journal of Clinical Biomechanics 21, S3-S8.

Wu, G., Siegler, S., Allard, P., Kirtley, C., Leardini, A., Rosenbaum, D., Whittle, M., D'Lima, DD., Cristofolini, L., Witte, H., Schmid, O., Stokes, I., 2002. ISB recommendation on the definitions of joint coordinate systems of various joints for the reporting of human joint motion-part I: ankle, hip, and spine. Journal of Biomechanics 35, 543-548.

Wu, G., van der Helm, F., Veeger, H., Makhsous, M., Roy, P., Anglin, C., Nagels, J., Karduna, A.R., McQuade, K., Wang, X., Werner, F.W., Buchholz, B., 2005. ISB recommendation on the definitions of joint coordinate systems of various joints for the reporting of human joint motion-Part II:shoulder, elbow, wrist and hand. Journal of Biomechanics 38, 981-992.

Figure Legends

Figure 1 The JCS mobile square-window (on the right shoulder)

(a) arbitrary GHJ orientation (b) GHJ neutral position (c) primarily abducted humerus with coupled flexion, β=α-90 (d) primarily flexed humerus with coupled abduction, θ=φ-90.

$\mathbf{u}_{sz}$: a medio-lateral line through the spine root; $\mathbf{u}_{sy}$: a cross-product of $\mathbf{u}_{sz}$ and a line through the ridge of the lateral border; $\mathbf{u}_{sx}$: the cross-product of $\mathbf{u}_{sy}$ and $\mathbf{u}_{sz}$; $\mathbf{u}_{hy}$: the cross-product of the humeral canal axis $\mathbf{u}_{hx}$ and 'a line directed from the surface area centriod of the medial epicondyle to that of the lateral epicondyle'; $\mathbf{u}_{hz}$: the cross-product of $\mathbf{u}_{hy}$ and $\mathbf{u}_{hx}$ (Amadi et al., 2008; Amadi et al., 2009a).

Figure 2 (a) arbitrary right humeral position, (b) decomposing flexion, (c) abduction and (d) rotation

Figure 3 JCS kinematics corresponding to arm elevation in three planes (Converted from Fung et al, 2001); A: Coronal, B: Scapular and C: Sagittal plane humeral elevations

Table 1 Range-of-motion (ROM) arm elevation in the coronal, scapular and sagittal planes showing the true humeral bearing quantified anteriorly from the image coronal plane of the Visible Human Female.

Table 1

	Humeral long axis bearing anteriorly from the image coronal plane(°)		
ROM arm elevation (°)	Coronal	Scapular	Sagittal
0	xxxx	xxxx	xxxx
20	xxxx	xxxx	xxxx
30	-46.9	51.2	71.8
40	-37.6	43.9	71.6
50	-29.3	37.6	71.5
60	-22.6	32.3	71.8
70	18	29	72.7
80	19.2	28.3	73.8
90	23.2	30.3	74
100	28.1	33.7	74.9
110	32.1	36.3	74.7
120	36.4	39	73.7
130	39.5	40.9	71
140	xxxx	xxxx	xxxx
150	xxxx	xxxx	xxxx
average	5.5	36.6	72.9
std	32.5	7.0	1.4

Figure 1

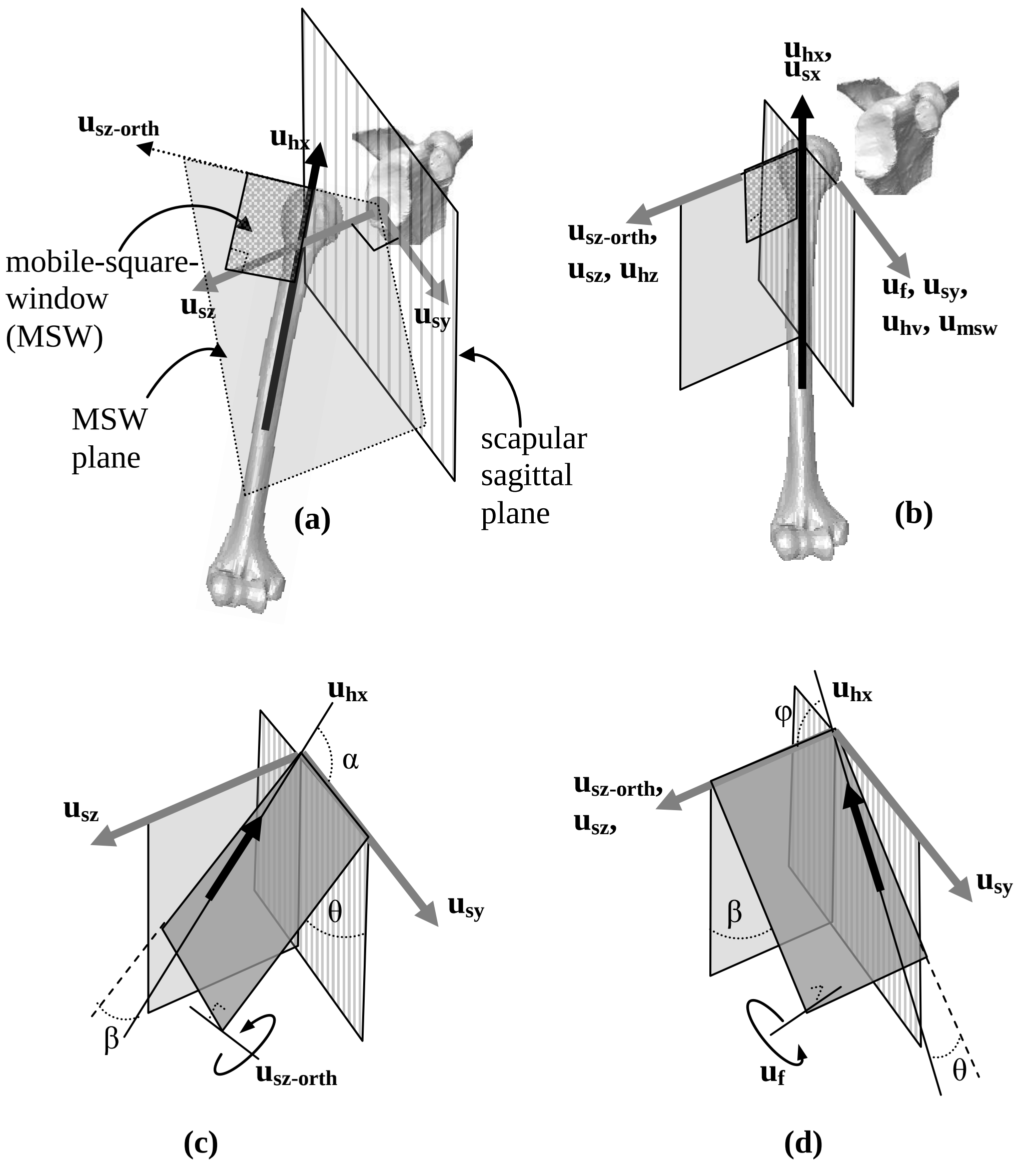

u_sz-orth
u_hx
mobile-square-
window
(MSW)
u_sz
u_sy
MSW
plane
scapular
sagittal
plane
(a)
u_hx,
u_sx
u_sz-orth,
u_sz, u_hz
u_f, u_sy,
u_hv, u_msw
(b)
u_hx
α
u_sz
u_sy
θ
β
u_sz-orth
u_hx
φ
u_sz-orth,
u_sz,
u_sy
β
u_f
θ
(c)
(d)

Figure 2

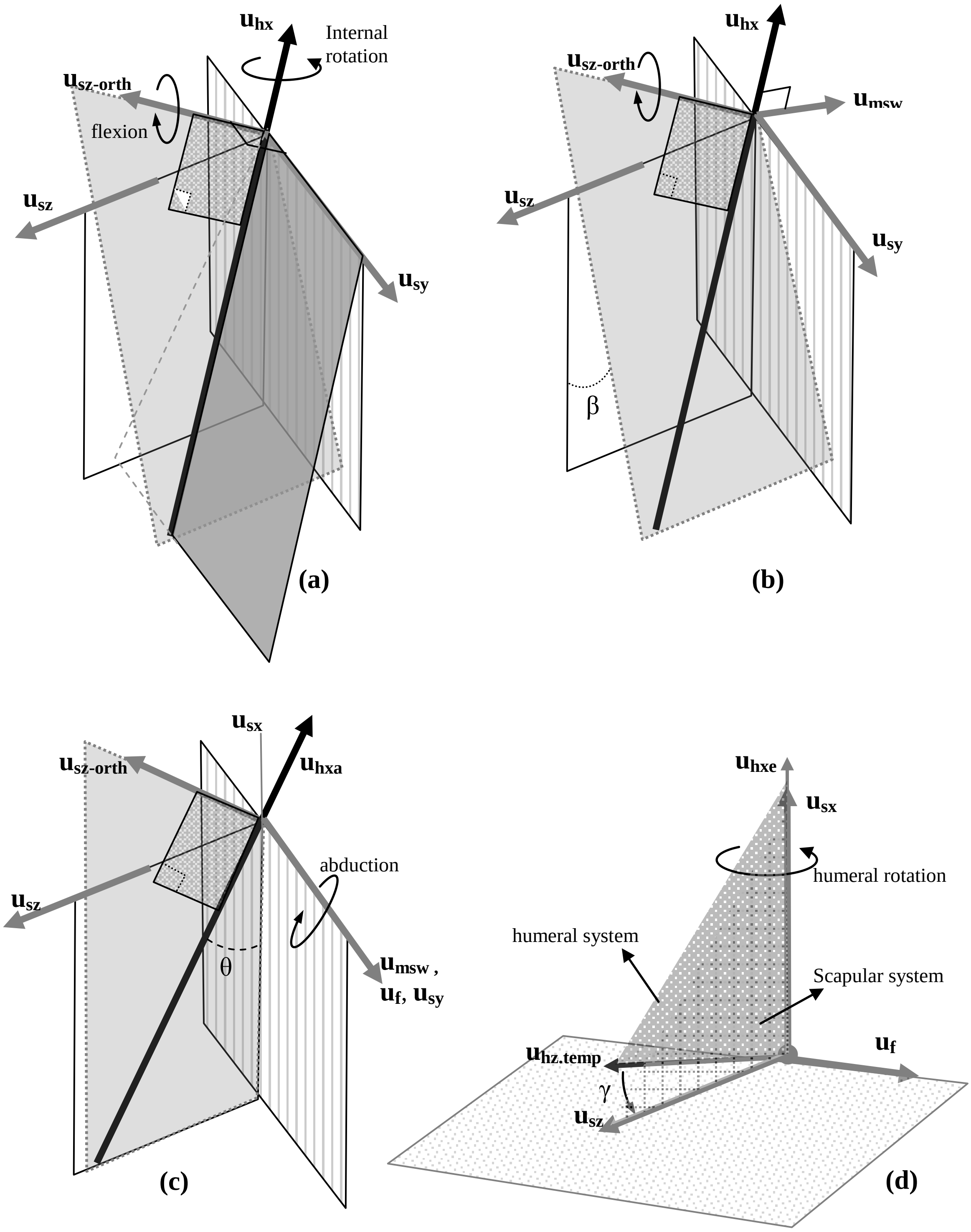
u_hx
Internal
rotation
u_sz-orth
flexion
u_sz
u_sy
(a)
u_hx
u_sz-orth
u_msw
u_sz
u_sy
β
(b)
u_sx
u_sz-orth
u_hxa
u_sz
abduction
θ
u_msw ,
u_f, u_sy
(c)
u_hxe
u_sx
humeral rotation
humeral system
Scapular system
u_f
u_hz.temp
γ
u_sz
(d)

Figure 3

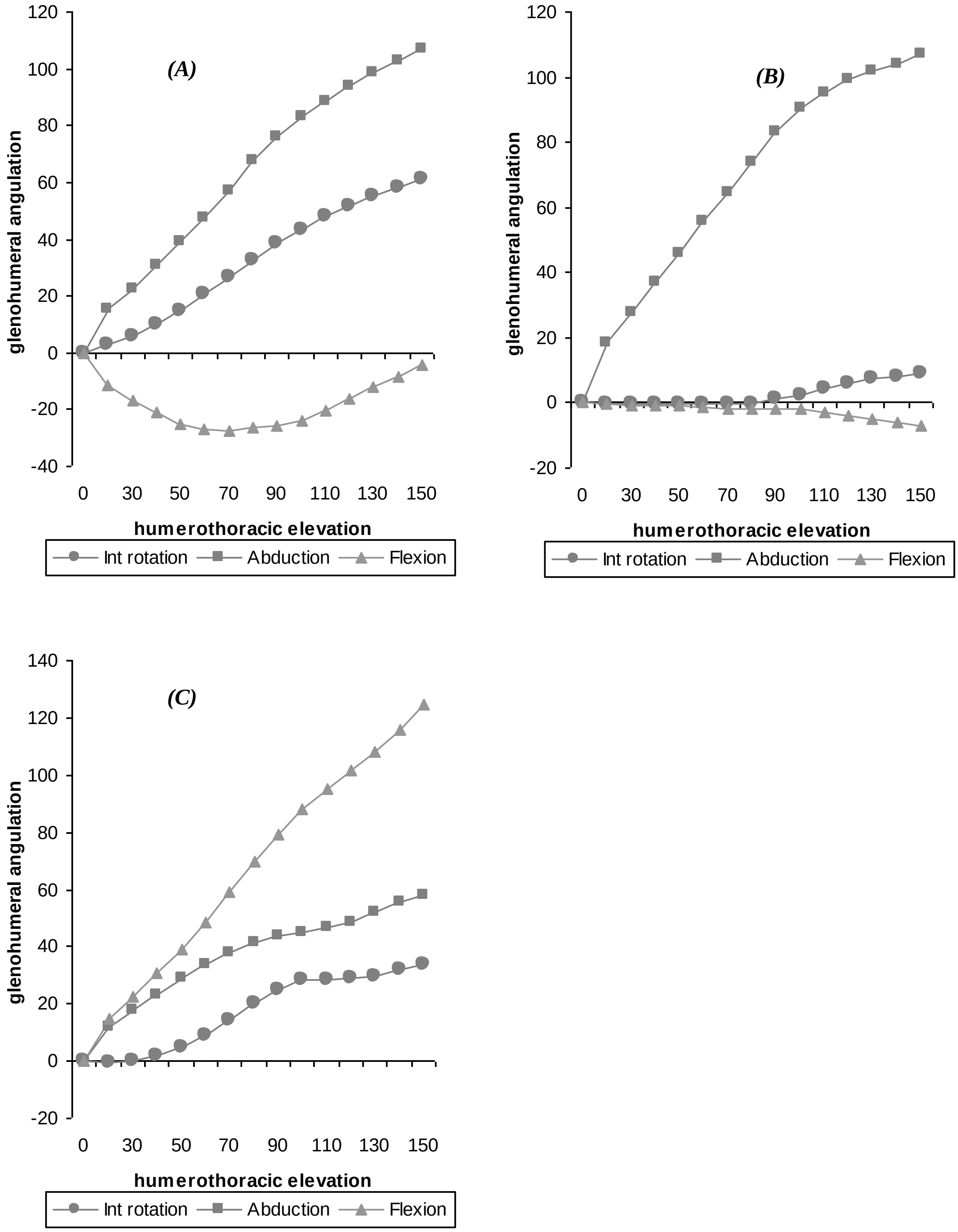

(A)
glenohumeral angulation
120
100
80
60
40
20
0
-20
-40
0 30 50 70 90 110 130 150
humerothoracic elevation
Int rotation
Abduction
Flexion
(B)
glenohumeral angulation
120
100
80
60
40
20
0
-20
0 30 50 70 90 110 130 150
humerothoracic elevation
Int rotation
Abduction
Flexion
(C)
glenohumeral angulation
140
120
100
80
60
40
20
0
-20
0 30 50 70 90 110 130 150
humerothoracic elevation
Int rotation
Abduction
Flexion